



Impacts of a floating photovoltaic system on temperature and water quality in a shallow tropical reservoir

Peipei Yang¹ · Lloyd H. C. Chua² · Kim N. Irvine³ · Manh Tuan Nguyen⁴ · E.-Wen Low⁵

Received: 20 May 2021 / Accepted: 1 June 2022 / Published online: 3 July 2022
© The Author(s) 2022

Abstract

A three-dimensional hydrodynamic-ecological lake model combined with field measurements and sampling was applied to investigate the impacts of floating photovoltaic (PV) systems on hydrodynamics and water quality in a shallow tropical reservoir in Singapore. The model was validated using field data and subsequently applied to predict temperature and water quality changes for a hypothetical 42 ha placement of floating photovoltaic panels, covering about 30% of the water surface and capable of generating up to 50 MW of energy. The impact of the panel placement was studied numerically. The area of the reservoir where panels are placed experiences both light limiting and reduced wind stress conditions. The model indicated an average water temperature increase of 0.3 °C beneath the panels, consistent with the field observation from a 1 ha demonstration installation. Comparisons of model results between the uncovered and covered areas reveal greater stability of the water column (increase in Richardson number from 2.3 to 3.3) and reduction in mixing energy (from 9×10^{-7} to 7×10^{-7} W/kg) under the PV panels. Furthermore, the model predicted that chlorophyll *a*, total organic carbon and dissolved oxygen concentrations would decline by up to 30%, 15% and 50%, respectively, under the photovoltaic panels. Total nitrogen and total phosphorus, averaged over the water column, increased by 10% and 30%, respectively, under the panels. Distant from the floating solar panels, temperature, stability and water quality were unaffected.

Keywords Field measurements · Floating solar panels · Numerical model · Reservoir management · Shallow tropical reservoir · Water quality

Introduction

Photovoltaic (PV) power generation is one of the renewable energy sources that has received increasingly widespread interest, with global capacity experiencing a tenfold increase in the 5 years prior to 2014 (Ellabban et al. 2014), while 2015 saw a 28% increase in capacity, which was greater than any other renewable energy source (REN21 2016). However, utility-scale PV plants are land intensive and as a result, some countries including China, Singapore, Japan, South Korea and the Philippines are starting to investigate the use of floating PV systems installed in lakes and reservoirs (Sahu et al. 2016; Harvey 2016; Hanwha 2017). The application of floating photovoltaic (PV) systems as a source of renewable electrical generation has been gaining popularity recently with capacity increasing worldwide by 50%, reaching over 74 GW between 2016 and 2017 (IEA 2017). China, which is one of the largest users of this technology, has a 40 MW floating PV system in Anhui province and is building a 150 MW facility in the same province (IEA 2017).

✉ Lloyd H. C. Chua
lloyd.chua@deakin.edu.au

¹ EPMC Centre, Nanyang Environment and Water Research Institute (NEWRI), Nanyang Technological University (NTU), Singapore, Singapore
² School of Engineering, Faculty of Science Engineering & Built Environment, Deakin University, 75 Pigdons Road, Waurn Ponds, VIC 3216, Australia
³ Faculty of Architecture and Planning, Thammasat University, Rangsit Campus, Khlong Luang, Pathum Thani 12121, Thailand
⁴ Water Quality Department, PUB, Singapore's National Water Agency, 80 Toh Guan Rd E, Singapore 608575, Singapore
⁵ Catchment and Waterways (Reservoir Management Division), PUB, Singapore's National Water Agency, 40 Scotts Road Environment Building, Singapore 228231, Singapore

Japan, the UK and South Korea also are building floating PV systems with capacities ranging from 6.3 to 100 MW (Boyd 2016; Hanwha 2017; Harvey 2016).

Floating PV systems offer at least 2 important advantages over land-based PV systems. Firstly, traditional PV farms are land intensive and in countries with limited land space, floating PV offers a viable alternative. Secondly, floating PV systems generally have a higher generation efficiency as compared to land-based PV systems due to the cooling effect of the water body. Sahu et al. (2016) reported that floating PV installations have on average, an 11% higher generation efficiency due to cooler temperatures over the water surface, while Trapani and Redon-Santafe (2015) indicated that for a demonstration project in Italy, a 20 to 25% increase in efficiency was observed. Zsiborács et al. (2016) note that the generation efficiency generally decreases by 0.5% with each 1 °C increase in temperature. Notwithstanding these advantages, however, a rigorous quantitative study on the impact of shielding by such floating systems on hydrodynamics and water quality is lacking. Such studies are essential if the installation of PV systems is to be done in an environmentally sustainable way, and at the same time optimizing power generation.

Floating PV systems block solar radiation and reduce wind stress at the water surface. The almost complete reduction in shortwave (SW) radiation by the PV panels can affect both the heat balance and light penetration into the water column. The surface water temperature is expected to decrease due to shading of PV panels, although the water surface also can be warmed by thermal radiation from the panels and the reduction of evaporative heat flux at the water surface. The net result of these competing mechanisms is as yet unknown. In addition, the influence of shading on reservoir water temperature is a function of the ratio of the shading area to the water body, where the impacts of the shading on water temperature in small- or medium-sized water bodies tend to be more significant than in larger water bodies (Boothroyd et al. 2004; Davies-Colley and Quinn 1998). Reduced light intensity by PV systems can be the overriding factor controlling algal growth even in the presence of sufficient nutrient supply. Under light limiting conditions, photosynthesis by phytoplankton is inhibited and respiration is dominant (Huisman et al. 2004). Various studies (Chen et al. 2009a; Ghermandi et al. 2009) have shown that shading can effectively reduce algal biomass by about 50%, in small- or medium-sized water bodies such as Lake Taihu, China, and Nete River basin, Belgium, both of which suffer from harmful algal blooms. When photosynthesis is inhibited, DO production will be reduced (Chen et al. 2009b), and with respiration ongoing, DO is depleted.

The reduction in wind stress and the formation of an artificial microclimate in the air space between the panels and lake surface alters the energy transfer process between

the atmosphere and lake (Oswald and Rouse 2004). Spatial heterogeneity of the wind field on the water surface can lead to modification of flow patterns and mixing (Xing et al. 2018). The introduction of a microclimate results in an alteration of sensible and latent heat fluxes, both of which are important components of the energy budget for a lake. There also may be synergistic effects, for example, as sensible heat and latent heat are affected by wind speed. Hipsey et al. (2004) observed substantial reduction in sensible and latent heat flux when the water surface was sheltered from wind compared to when it was unsheltered. Coupled with the potential for the panels to heat the water surface directly, this may cause warming of the near surface water. Lake mixing processes and mass transport depend on mixing energy (Fischer 1979). The placement of the solar panels on the water surface will lead to reduced wind speed increasing the potential for weaker vertical mixing in the lake. As a result, vertical exchange may be inhibited, negatively impacting the mass and heat transport through the water column (Yin et al. 2004). In addition, an inhomogeneous wind field could cause changes to mass exchange rates in connected basins. Rueda et al. (2005) examined the inter-basin exchange rate using numerical tracer experiments and reported that the flushing time under a uniform wind field was different from that under a spatially varied wind field.

Singapore is exploring the use of its reservoirs to support floating PV systems (PUB 2017). A 1 ha test bed facility was installed in the Tengeh Reservoir (Boh 2016) with plans to expand its capacity to 50 MW, covering one-third the reservoir's surface area (Soh 2017). Plans are also underway for additional floating systems of up to 1.5 MW to be installed at other reservoirs in the country (PUB 2018). Determination of the net effects of shielding, the microclimate layer and reduction in wind stress on water temperature and quality is complex, and its importance warrants detailed studies. Such an environmental impact assessment is of social importance, especially for drinking water reservoirs, which, to the best of our knowledge, has not been undertaken. The closest study relevant to this paper can be found in Haas (2020), who used a similar three-dimensional (3D) modelling approach to assess ecological impacts in a hydropower application; however, no measurements were reported to support their model results. The objectives of this research were therefore to: (i) examine changes to radiation fluxes at the water surface when covered by solar panels; (ii) compare stability and water quality in the water column below the solar panels and in open water; (iii) make predictions of the water quality for a hypothetical installation of a 30 MW floating solar PV system at prototype scale; and (iv) illustrate how our combined opportunistic sampling, continuous monitoring and modelling can provide a benchmark framework to assess environmental impacts due to floating PV systems. The scope of our study involved both field sampling in the

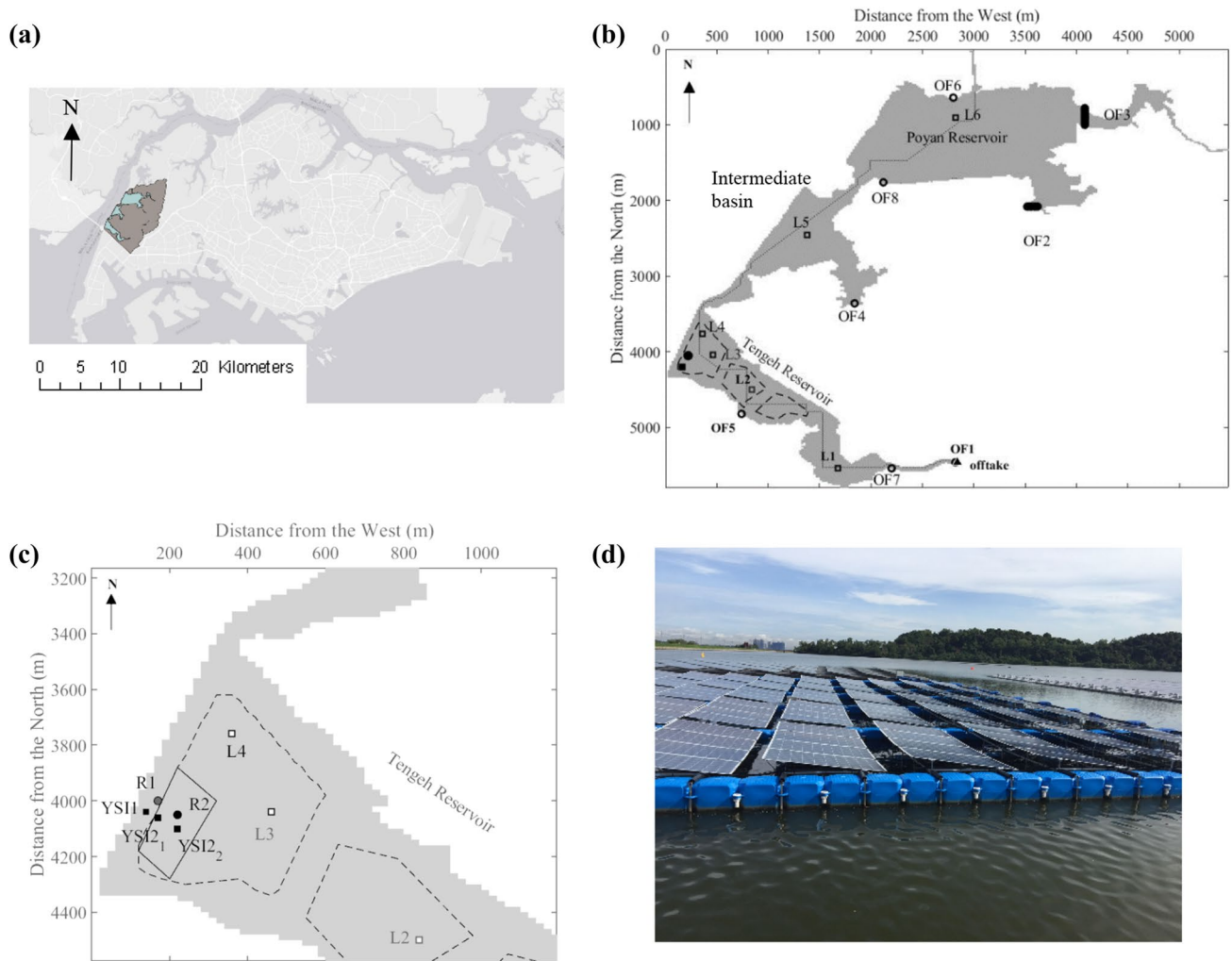


Fig. 1 (a) Location map of Tengeh and Poyan Reservoir catchments in Singapore. (The reservoir is highlighted in blue.) (b) Locations of manual sampling sites (L1–L6), planned 42 ha prototype floating PV installation (enclosed by dashed lines) and longitudinal transect (dotted line) for model result visualization. OF1–OF6 represent locations

of stormwater runoff outfalls, (c) close-up showing locations of YSI and radiometer (*R*) measurements, and the 1 ha demonstration-scale panel (solid line) and planned installation area of 42 ha prototype (dashed line) system. (d) Photograph showing the 1 ha demonstration-scale floating PV panels installed on site

Tengeh–Poyan Reservoir system, Singapore, in 2016 and numerical modelling with a 3-D hydrodynamics and water quality model. The results from field sampling provided data for model validation. The numerical model was then used to predict potential impacts on hydrodynamics and water quality for a hypothetical 30 MW (42 ha) prototype-scale installation. Further monitoring was conducted with the installation of a 6 m² mock-up, and a 1 ha demonstration-scale floating solar PV system installed in Tengeh Reservoir in 2017, to assess changes to water quality under the panel, compared to open water conditions. The results from this study will be used to guide the design of a field-scale system and direct water quality monitoring plans as part of the operation of the floating PV system.

Methods

Study site

The study was conducted in the Tengeh and Poyan Reservoirs located in the western part of Singapore (Fig. 1a). The two reservoirs are shallow and separated by an intermediate basin. The total contributing catchment is approximately 25.6 km² and is predominantly forested (83%), while a proportion of the remaining area is a combination of residential, institutional and agricultural land uses. Singapore experiences a tropical rainforest (Af, Köppen climate classification) climate with high levels of solar radiation, air temperature and humidity. Figure 2 shows that the daily air temperature typically increases to

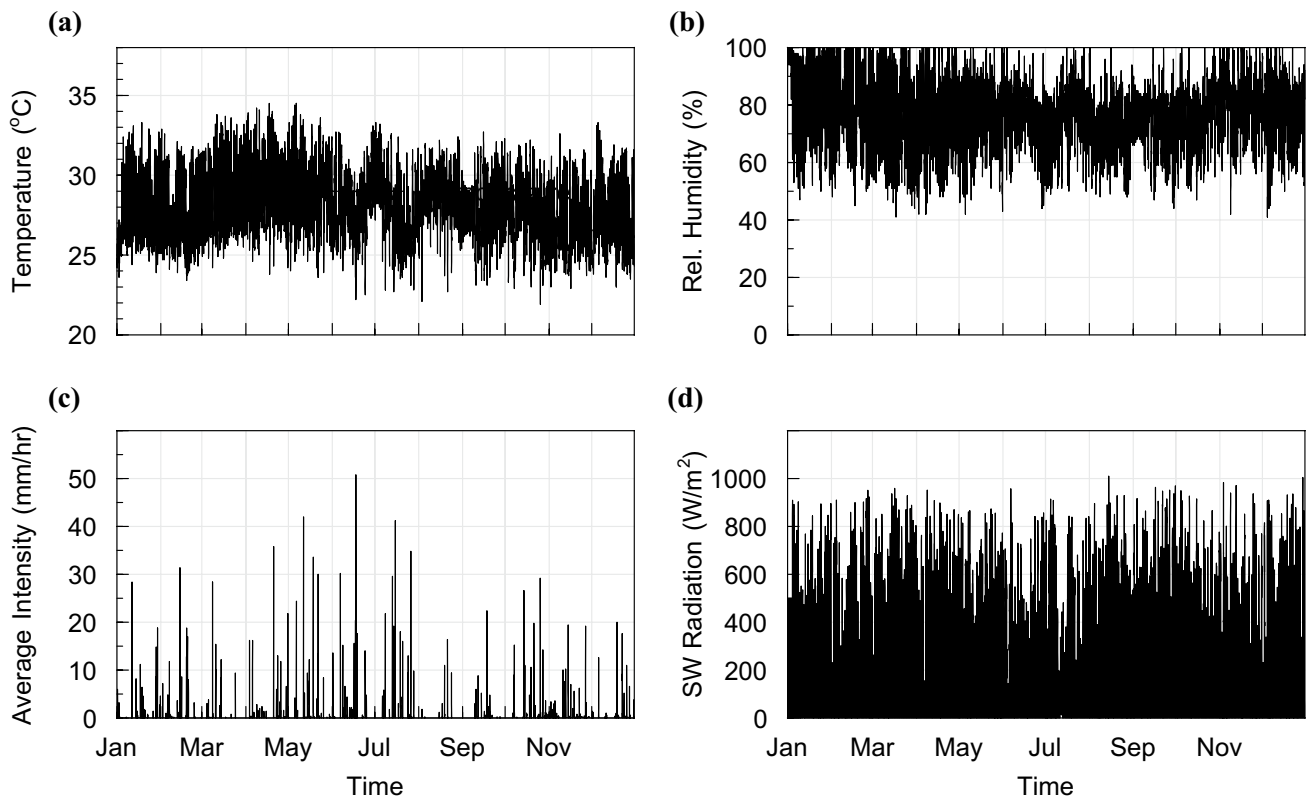


Fig. 2 (a) Air temperature, (b) relative humidity, (c) average rainfall intensity, and (d) shortwave radiation at the study site for 2016

32 °C in the daytime accompanied by modest wind speeds of about 2 to 6 m/s, and the night-time air temperature drops to about 26 °C on average with generally weaker wind speeds (data collected from Changi Meteorological Station, The National Environment Agency, Singapore). Climate is governed by 2 distinct monsoon seasons in a year: the NE monsoon season from January to April and the SW monsoon season from June to October (NEA 2016). Although rainfall is present throughout the year, the wet period lasts from December to January and the annual rainfall averages about 2500 mm (Fig. 2).

Field studies

Field monitoring and sampling were conducted over a 24 month period from May 2015 to May 2017. The field-work carried out included longer-term opportunistic sampling, as well as short-term continuous monitoring and radiation measurements.

Opportunistic sampling

Surface water samples were collected at 6 monitoring sites for the opportunistic sampling campaign. Sites L1 to L4 are

located in Tengeh Reservoir, L5 in the intermediate basin between Tengeh and Poyan and L6 in Poyan Reservoir (Fig. 1b). The 1 ha demonstration-scale floating solar system was installed at one end of the Tengeh Reservoir (Fig. 1c). Sampling locations L2, L3 and L4 are within the hypothetical 42 ha prototype-scale installation, while L1, L5 and L6 are outside the 42 ha area. Water samples were collected manually from 0.5 m below the water surface and tested for TSS, TOC, DOC, NH₃-N, NO_x-N, TN, PO₄-P, TP and chlorophyll *a* at an accredited laboratory. Samples were collected and preserved following standard methods (APHA 2005). Field sampling was conducted in 2016 to provide data for model validation, initially at quarterly intervals, increasing to fortnightly in the latter part of 2016. Chlorophyll *a* data were augmented by sampling data from the Public Utilities Board, which manages the reservoir.

Continuous monitoring

A demonstration-scale, 1 ha floating solar PV system (Fig. 1c, d) with maximum 1 MW of energy production (PUB 2017) was installed in Tengeh Reservoir between July and September 2016, allowing for water quality and radiation data to be collected under the panels. Continuous monitoring took place in 2017 using two YSI 6920

datasondes (YSI.com), which were installed 0.8 m below the water surface both in open water (distant from the floating PV locations) and beneath the panels.

The YSIs provided continuous measurements of water temperature, DO and pH over a limited time period at locations YSI1, YSI2₁ and YSI2₂ (Fig. 1c). One YSI was suspended from a boardwalk at location YSI1 away from the demonstration panels representing open water conditions between 28 November 2016 and 12 July 2017. Another YSI was placed at location YSI2₁ under a 6 m² mock solar panel structure adjacent to the 1 ha demonstration system from February to 25 March 2017 and then shifted to the location YSI2₂ in the centre of the 1 ha demonstration system from 21 June to 12 July 2017, representing conditions in the water column under the solar panels. Placing the YSI datasondes beneath the 6 m² and 1 ha size PV systems allowed scale effects to be studied. Data were continuously logged at 15 min intervals and downloaded on a weekly basis. The resolution of the temperature sensor is 0.01 °C, and the accuracy is ± 0.15 °C. The resolution of the DO sensor is 0.01 mg/l with an accuracy of ± 0.1 mg/l. The resolution of the pH sensor is 0.01 unit with an accuracy of ± 0.2 unit. All sensors were calibrated prior to installation and serviced weekly. The DO sensor was re-calibrated as part of the weekly maintenance schedule (Irvine et al. 2005).

Radiometer measurements

Two radiometers (Kipp & Zonen CNR4 Net Radiometer) were used to continuously log air temperature and radiation at 10 min intervals from 16 February 2017 to 30 November 2017 under the 1 ha demonstration-scale floating PV system. The radiometers consisted of a pair of pyranometers, one facing upward and the second facing downward and a pair of pyrgeometers, oriented similarly, allowing the energy balance between incoming SW and longwave (LW) radiation versus surface-reflected SW and outgoing LW radiation to be measured. A temperature sensor was integrated with the radiometer to correct the longwave radiation readings by accounting for the temperature of the instrument housing. A second temperature measurement was made for the ambient air temperature. Radiometer R1 (Fig. 1c) was placed away from the panels to represent ambient or open water conditions, and R2 (Fig. 1c) was placed directly beneath a solar panel in the middle of the 1 ha demonstration system (in the same area as YSI2₂) to represent the microclimate or below panel conditions.

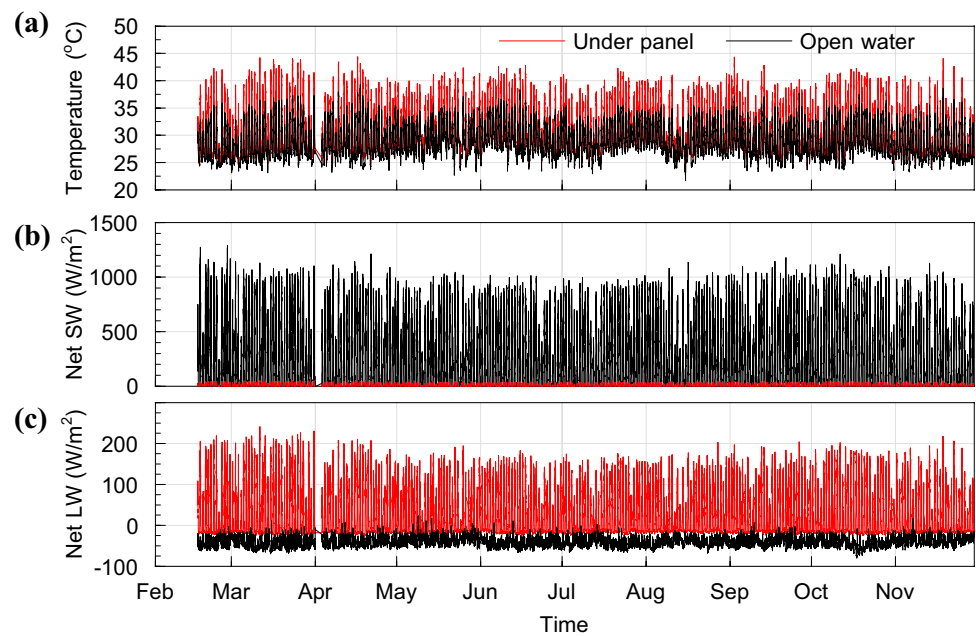
Numerical modelling

A 3D Estuary, Lake and Coastal Ocean Model—Computational Aquatic Ecosystem Dynamics Model or ELCOM-CAEDYM (ELCD), was used for reservoir modelling. Recent applications of the model to other reservoirs in Singapore include studies by Xing et al. (2018) and Yang et al. (2019a). ELCOM solves the unsteady, hydrostatic, Boussinesq, Reynolds-averaged Navier–Stokes (RANS) equations using a mixed-layer model to simulate the mixing process in the vertical water column (Laval et al. 2003). The surface thermodynamics in ELCOM treats the system as discrete changes to the temperature structure in the upper grid cells rather than as boundary conditions for transport or mixing equations. The heat transfer changes the density stratification, either providing turbulent kinetic energy (TKE) available (unstable density gradients produced by net cooling) or increasing to overcome stratification. Once a new density field is calculated, the mixing process is modelled on a layer-by-layer basis through each layer by comparing the TKE available from convective overturns, shear production, wind stirring and converting excessive TKE from the previous layer to the potential energy that is required to mix a grid cell up into the mixed layer above.

The CAEDYM model includes comprehensive process representation of the C, N, P and DO cycles, as well as several classes of inorganic suspended solids, and phytoplankton dynamics. Both the inorganic and organic and dissolved and particulate forms of C, N and P are modelled explicitly along the degradation pathway of POM to DOM to dissolved inorganic matter (DIM). The nitrogen cycle includes the additional processes of denitrification, nitrification and N₂ fixation that are not in the carbon and phosphorus cycles. DO dynamics within the CAEDYM model include atmospheric exchange, sediment oxygen demand (SOD), microbial use during organic matter mineralization and nitrification, photosynthetic oxygen production and respiratory oxygen consumption and respiration by other optional biotic components. To model the phytoplankton biomass (TChla), the maximum potential growth rate can be set as a user-defined temperature and be multiplied by a temperature function considering light and nutrient limitations. Three phytoplankton groups were considered in the estimation of TChla, dinoflagellates and two cyanobacteria groups (*Anabaena* and *Nodularia*). Phytoplankton may also be grazed upon by zooplankton, and fish. CAEDYM is dynamically coupled with ELCOM to model 3D transport and interactions of flow physics, biology and chemistry (Leon et al. 2011). The CAEDYM model was run at the same 2 min time step as the hydrodynamic model to resolve sub-daily algal processes (diurnal photosynthesis and nocturnal respiration).

Bathymetry data were provided by PUB, Singapore's National Water Agency. Other inputs for the ELCD model

Fig. 3 (a) Air temperature, (b) shortwave radiation and (c) longwave radiation measured under the 1 ha demonstration-scale floating PV panel for 2017



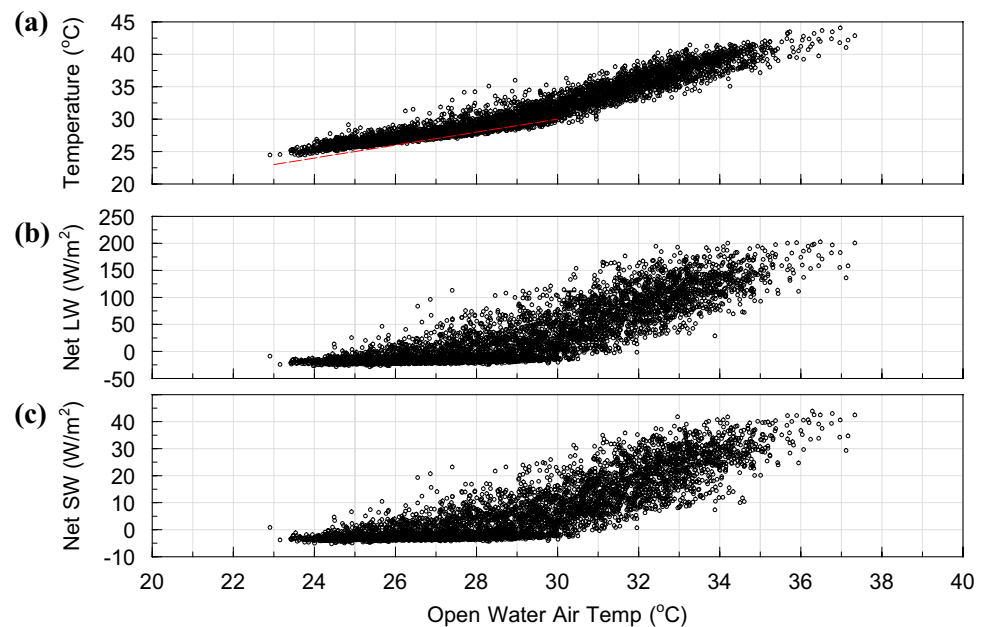
included radiometer and temperature measurements under the panels and meteorological data including SW and LW radiation, rainfall, air temperature, relative humidity, wind speed and wind direction, which were provided by the National Environment Agency, Singapore (NEA). Inflow quantity and quality time series data were obtained from a catchment model, PCSWMM, which employs the US EPA SWMM5 computational engine, but includes a graphical user interface that sits within a GIS-based platform. SWMM (Stormwater Management Model) has been applied globally and is an industry standard model (Jayasooriya and Ng 2014; Irvine et al. 2015; Niazi et al. 2017; Song and Chung 2017). The PCSWMM model was calibrated using flow and water quality measured at 4 monitoring locations within the catchment, and the calibration was then extended to ungauged parts of the catchment to provide catchment wide flow and nutrient loadings into the reservoir. Water quality data for a total of 21 rain events were used for calibrating the build-up/washoff water quality model in PCSWMM (with 10 additional events being used for validation), while continuous flow data were used for calibrating the runoff model. Details and results from the catchment model are not shown here and will be reported separately.

The reservoir model was validated using the data collected from the opportunistic sampling study conducted in 2016, prior to panel installation, applying the meteorological data obtained from the NEA at the surface boundary. An autoregressive model was used to fill in gaps (Akaike 1969) in the shortwave radiation data in the months of March–April. Two floating monitoring stations at L1 and L6 (Fig. 1b) in Tengeh Reservoir and Poyan Reservoir, respectively, installed by the PUB provided continuous surface

water temperature measurement which was used as a check on the model results. The computational grid used in the ELCD model contained 2.3×10^6 computational cells in a $20 \text{ m} \times 20 \text{ m}$ (horizontal) $\times 0.5 \text{ m}$ (vertical) mesh. The model was run with a time step of 2 min on a 9-node cluster computer with each node (Intel Xeon X5675, 3.07 GHz) consisting of 6 cores with 24 GB memory, taking approximately 60 h to complete a full year (1 January–31 December 2016) simulation.

The ELCD model was next run with the prototype 42 ha floating PV system placed on the water surface (Fig. 1b) and run for 2016. Radiation data measured beneath the panels in the 1 ha demonstration panels were analysed to provide the net radiation input to the reservoir surface at the panel location. In addition to net radiation, relative humidity under the panel was estimated based on the correlation between relative humidity and air temperature in open water. Considering that the tilt angle and spacing between individual panels are small (Fig. 1d), we assumed that the surface is fully covered (no gaps between panels) and imposed zero wind condition on the water surface where the solar PV panels are placed. With these prescriptions of the meteorological forcings at the panel locations, the ELCD model was run for the 42 ha floating PV scenario, and changes to the water quality, with and without the PV system in place, were compared.

Fig. 4 Measurements taken in 2017 under the 1 ha demonstration-scale floating PV panel (a) air temperature (perfect agreement is indicated by a red dashed line), (b) net longwave radiation, and (c) net shortwave radiation. These data are plotted as a function of the open water air temperature



Results

Radiometer measurements

Air temperature (Fig. 3a) was greater beneath the panels during the daytime (07:00 h–19:00 h) and cooled to slightly above ambient air temperature at night (19:00 h–07:00 h). Shortwave radiation was significantly reduced (Fig. 3b), as expected, due to shielding by the panels. The net LW radiation increased dramatically (Fig. 3c), as a result of thermal radiation by the panels. The net radiation balance (net LW + net SW), however, showed a reduction since the SW energy which forms the larger component of the energy budget is almost eliminated.

The radiation boundary condition at the water surface under the panels at the prototype scale had to be correctly prescribed in the numerical model. A fully physical approach to model the heat transfer between the PV panels, air layer and water surface is currently being developed. An empirical approach, however, was adopted in this study, using the measured data to provide estimates of the air temperature and radiative flux beneath the panels as a function of the open water air temperature. This approach is justified since conditions beneath the panels are driven by solar irradiance. The air temperature measured under the solar panels is increased significantly during the daytime, while in the night-time the air temperature decreased to nearly ambient conditions (Fig. 4a). The net radiation (Fig. 4b, c) approaches asymptotically to ambient condition in the night-time, since the solar panels were cooled to near ambient temperature with the absence of SW radiation. In the daytime, there is an increase in the net

LW radiation due to the heating from the panels, and SW radiation is significantly reduced due to shielding. The data (Fig. 4a–c) allow the development of relationships between the air temperature and net radiation beneath the panels as a function of the ambient air temperature, thus allowing a simplified approach to estimate the surface radiative flux boundary condition.

Continuous monitoring results

The water temperature data measured by the YSIs at 15 min time steps for open water are compared with water temperature under the 6 m² PV panel and 1 ha PV systems (Fig. 5a, b). The average water temperature beneath the panels was significantly higher ($p < 0.05$) than the average temperature in open water for both the 6 m² and 1 ha demonstration panels, based on a Z-test. These results indicate not only significant warming to the water layer below the solar panels, but also at least qualitatively (as measurements were not conducted at the same time), a scale effect, where greater warming was obtained under the 1 ha demonstration panels compared to the 6 m² PV panel. Simultaneous measurements of air and water temperatures beneath the 1 ha demonstration panels over a 2-week period, where only 1 rainfall event was recorded (23 June 2017), are shown in Fig. 6. The air temperature beneath the panels from the radiometer (R2 in Fig. 1c) measurements is consistent with trends in the water temperature measured by the YSI datasondes (YSI2₂ in Fig. 1c). Resulting from differences in the specific heat capacities between air and water, fluctuations in air temperature depart markedly from the mean, compared with water

Fig. 5 Data collected from YSI sonde measurements including surface water temperature, pH and dissolved oxygen both under the solar panels and in open water in 2017. **(a)** 6 m² PV panel (temperature), **(b)** 1 ha demonstration panel (temperature), **(c)** 6 m² PV panel (pH), **(d)** 1 ha demonstration panel (pH), **(e)** 6 m² PV panel (DO), open water DO data are not available and **(f)** 1 ha demonstration panel (DO)

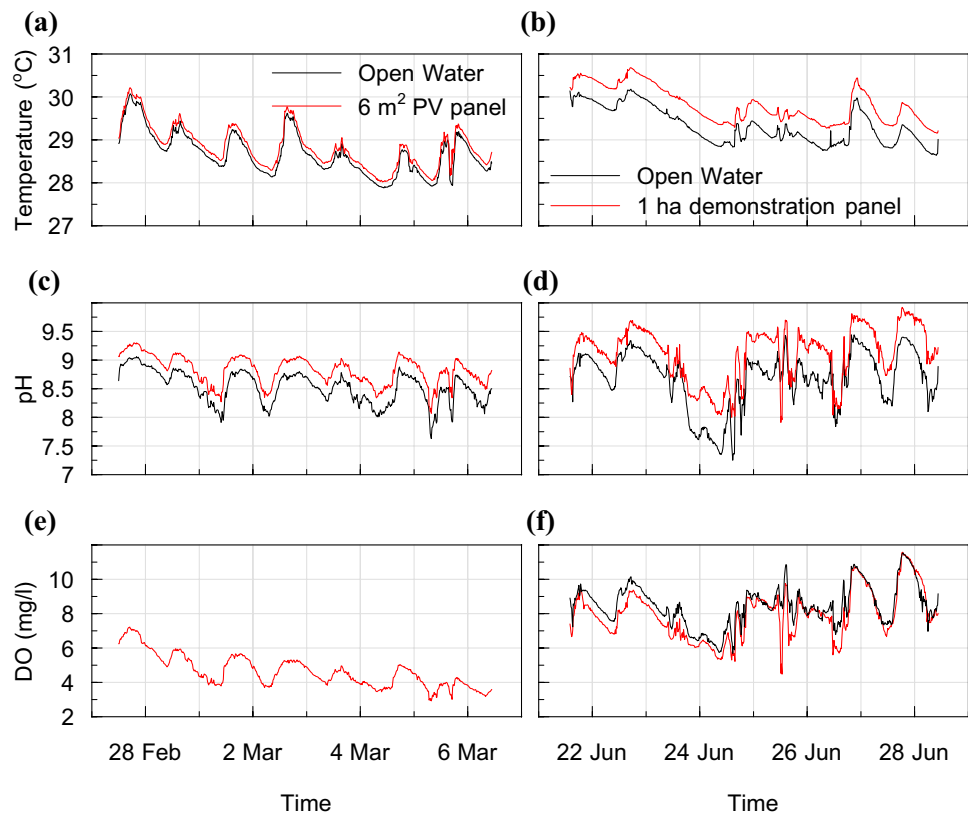
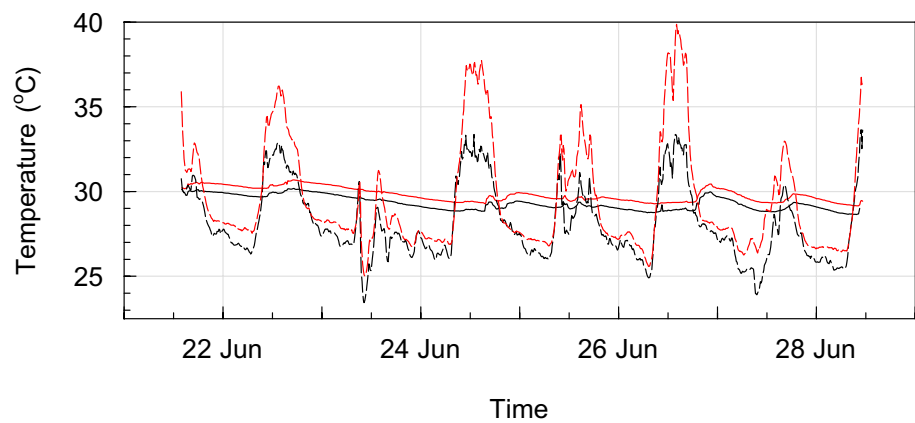


Fig. 6 Comparison of air and water temperature in open water and below 1 ha demonstration panels in 2017. Open water data are plotted in black and under panel data in red, air temperature data are plotted as dashed lines and water temperature data are plotted as solid lines

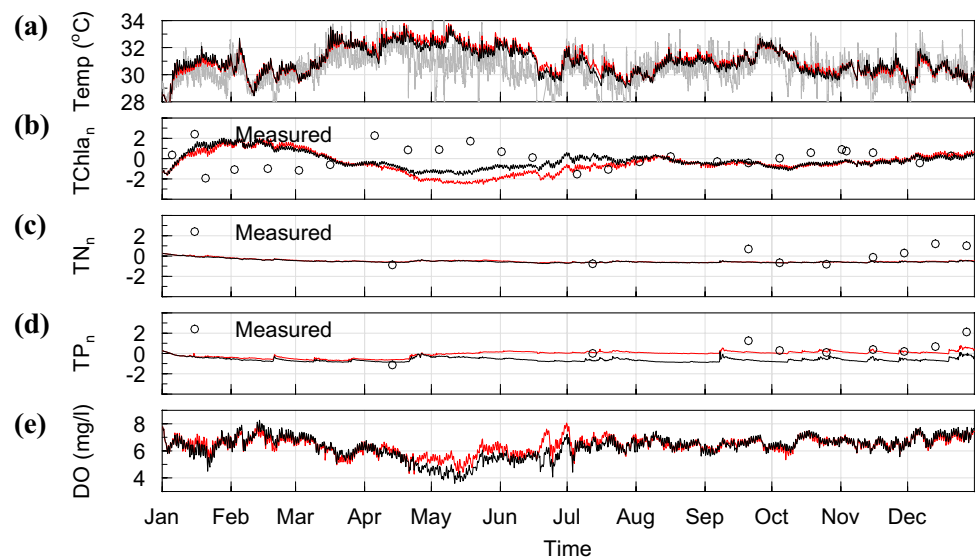


temperatures, and there is a lag in the peaks of water and air temperatures. The heavy rainfall (and increased cloud cover) at around noon on 23 June 2017 resulted in a poorly defined midday peak in air and water temperatures.

Further comparisons of the time series for other physico-chemical water quality indicators measured by the YSI datasondes are also provided (Fig. 5c–f). The measurements under the 6 m² PV panel (YSI2₁) and under the 1 ha demonstration-scale solar panels (YSI2₂) both indicate an increase of pH compared to open water measurements. Although the measurements under the 6 m² PV panel and

1 ha demonstration-scale systems were not carried out at the same time for direct inferences to be made, it can be observed that the increase in pH under the 1 ha demonstration panels, similar to surface temperature, is larger than for the 6 m² system in comparison with open water conditions. It is also observed that DO is lower under the 1 ha panel than in open water. The saturation concentration of DO is 111%, and DO is 8.48 mg/l in open water, while the saturation concentration is 105% and DO is 7.96 mg/l under the 1-ha demonstration-scale floating PV panel.

Fig. 7 Model results at L1 in 2016 for (a) water temperature, (b) normalized TChla, (c) normalized TN, (d) normalized TP and (e) DO. Open water and under panel data are in black and red, respectively (all figures), water temperature measurements are in grey (a), and other measured data are plotted as circles (b–d)



Discussion

Comparison of model results with field data

The ELCD reservoir model was run for 2016, and where available, the model results are compared with the opportunistic sampling and continuously monitored data at L1 (Fig. 7a) and L6 (Fig. S5a). The modelled surface temperatures are compared to the continuously measured water surface temperature data. The R^2 and RMSE are 0.5 and 0.95 °C for L1 and 0.7 and 0.53 °C for L6. While comparisons at L6 are satisfactory; there is no significant difference between modelled temperature and measured temperature ($p < 0.05$), the model results for the temperature at L1 did not fit as well with the measured data. L1 is close to a large stormwater drain outfall, and it is presumed that the colder inflows from major storm events are not adequately captured in the catchment model, as suggested by dips in the temperature measurements in L1, especially in May and June 2016. However, the reasonable agreement at L6 provides an indication that the model is able to capture the surface heating dynamics well. The model result of surface temperature better matches the measurement in the second half year of 2016. In the first half of 2016, the modelled surface temperatures are slightly higher than the measurements during May and June when it was especially rainy with large storm events.

The numerical model was used to predict the temperature and water quality parameters for the surface layer at sites L1 to L6 (Fig. 7 and Figs. S1 to S5). The TChla, TN and TP data are normalized (denoted by subscript n) by the mean μ and the standard deviation σ of the measurements (Z score $Z = \frac{x-\mu}{\sigma}$). The modelled water quality results are in overall good agreement with the observations. For example,

the R^2 and RMSE for TN ranged between 0.43–0.77 and 0.008–0.020 mg/l, respectively, for sites L1 through L6, while the R^2 and RMSE for TP ranged between 0.53–0.91 and 0.004–0.020 mg/l, respectively, for sites L1 through L6. However, TChla is underpredicted for L6, but provides better comparison for L1 and L2. The slight reverse in trend in the first half of the year is likely linked to the worse prediction of temperature as mentioned earlier. Nevertheless, it is seen that the ELCD modelled TChla concentration is within the same range as the field sampling results at these locations. The TP and TN concentrations match well with observations except towards the end of the year where measurements show an upward trend that is not replicated by the model. Rainfall is highest towards the end of the year (<http://www.weather.gov.sg/climate-climate-of-singapore/>), and it is likely that the inflow nutrient loading is not as well predicted during these periods of intense rainfall. The calibration of the catchment water quality model is a challenge, and while it is typical to calibrate the model for an average condition, given the large variability in rainfall, the model accuracy especially for extreme events may be compromised. Despite these difficulties, the general trends in the data are reasonably captured by the model.

Predictions for 42 ha prototype-scale floating PV system

Empirical functions relating the open water air temperature with air temperature and net radiation beneath the panels were prescribed as boundary conditions to the water surface directly beneath the panel. The proposed solar panels (Fig. 1b) cover an area of 42 ha or about 30% of the total surface area of Tengeh Reservoir. The model results at L2, L3 and L4 (Figs. S1a, S2a and S3a), where the panels are

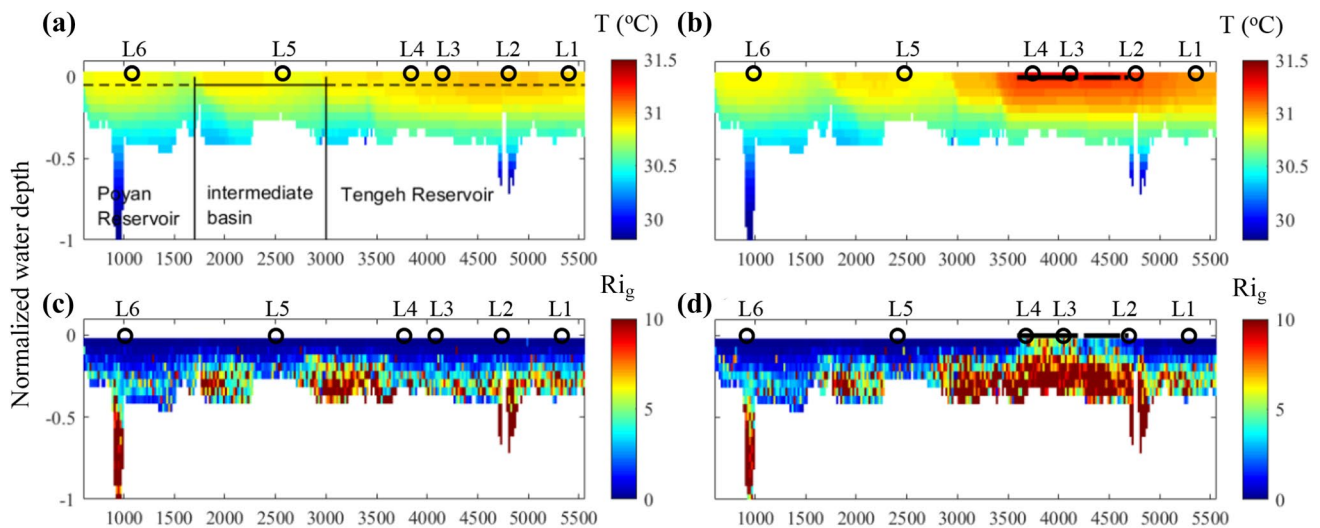


Fig. 8 Vertical and horizontal profiles of water temperature (a,b) and gradient Richardson number (c,d) with and without 42 ha floating PV panels, along the main axis of Tengeh and Poyan Reservoirs. The

solid black lines on the water surface adjoining L2 to L4 (b,d) represent approximate location of the floating PV panels

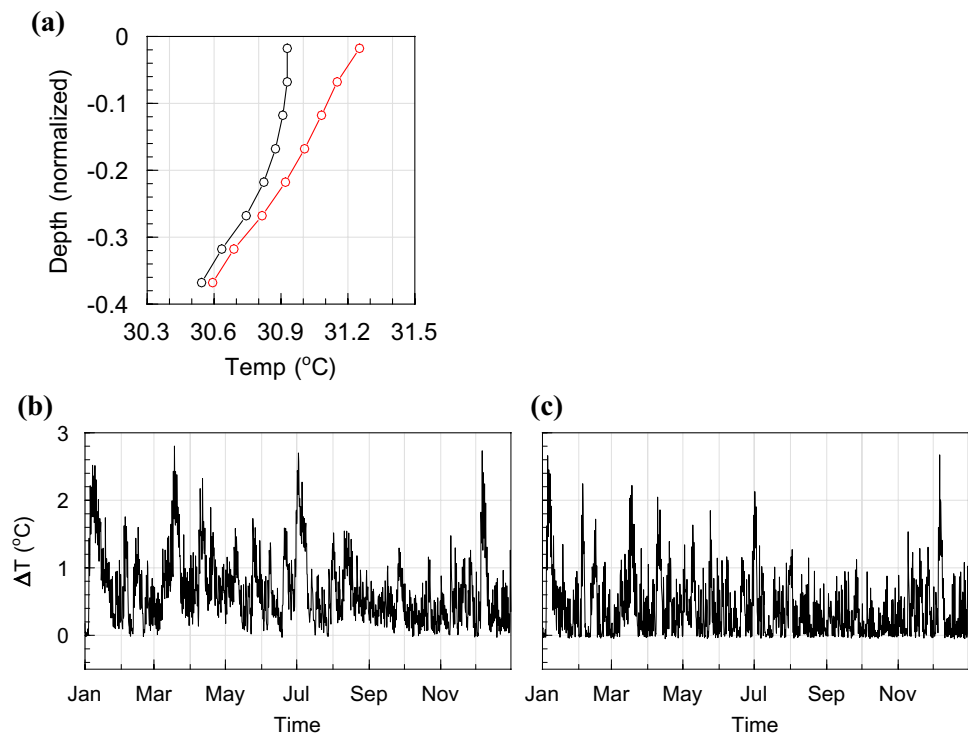
proposed to be installed, predicted that the surface water temperature under the panels would increase compared to open water conditions. An average increase of 0.32 °C in the daily mean water surface temperature is observed under the panels compared to open water conditions; the daytime temperature increase due to panel placement is estimated as 0.29 °C and the night-time temperature increase as 0.36 °C. The modelling results are roughly consistent with the YSI measurements where surface water temperature increases of 0.47 °C and 0.51 °C on average were observed under the 1 ha panel during the daytime and nighttime, respectively. This increase in water temperature is related to the increase in temperature of the air space between the PV panels and water surface, which was observed in our measurements (Fig. 3a). The increase in temperature in the air space is caused by conductive heating from the panels, as studies have shown that 13–20% of the solar radiation is converted into electricity and the remainder (> 80%) is converted into heat causing panel temperature to increase significantly (Armstrong and Hurley 2010). Our measurements showed a decrease in net radiation at the water surface beneath the panels (Fig. 3a, b). If only radiation energy was considered, it would suggest there should be a decrease in water temperature. However, the heat budget includes non-radiative latent heat and sensible heat (the latent and sensible heat are affected by wind speed, which we have assumed to be 0 m/s in the model) beneath the panels, as well as SW and LW radiation. It is the sum of these factors, under equilibrium conditions, which has important implications for surface water temperature (Yang et al. 2021).

It can be seen from the model results that TChla and TP concentrations and DO at L1 would also be affected by

the PV panels although L1 is close to the PV panel system (about 600 m away). As expected, there was no impact on temperature at L5 and L6 (Poyan Reservoir), since these locations are distant from the PV panels, about 1200 m and 2800 m away, respectively, and exchange of flow between the intermediate basin with Tengeh reservoir is limited by a narrow channel (close to L4, Fig. 1b).

The temperature depth profiles are compared, with and without panels (Fig. 8a, b). Depth is normalized by the maximum depth of the reservoir. In Tengeh Reservoir, the entire water column is heated as a result of panel placement. On the other hand, in Poyan Reservoir, there is virtually no difference in results. The water temperature profile, averaged over 2016, for L3 (Fig. 9a) indicates that the entire water column in Tengeh Reservoir would be heated with a temperature increase by about 0.3 °C at the surface, compared with open water, decreasing with depth to 0.05 °C at the bottom of the reservoir. On average, with the placement of panels, the surface–bottom temperature difference in the daytime is about 0.49 °C for open water and 0.70 °C under the solar panels, while the nighttime difference is 0.28 °C for open water and 0.61 °C under the solar panels. Although a change of < 1 °C may not seem large, given that the surface–bottom temperature difference in tropical reservoirs is typically in the order of 1 to 2 °C (Yang et al. 2019a, b), this increase in the vertical temperature difference throughout the day would result in a notable increase in stratification and stability conditions and alter the energy budget. The difference between surface and bottom water temperatures increases with the placement of the panels (Fig. 9a). It is also observed that water temperature increases monotonically, from the bottom, beneath the panels, compared to a mixed

Fig. 9 (a) Water temperature profile at L3 under the 42 ha prototype floating PV (red) and open water (black), averaged over 2016. Difference between the surface and bottom water temperatures (ΔT) (b) under the floating PV panels at L3 and (c) open water, for 2016



layer of uniform temperature extending to about mid-depth for open water conditions. The effect of panel placement on the vertical temperature gradient can also be observed from a comparison of the time series showing the difference between the top and bottom water temperatures (ΔT) with and without the floating PV panels (as indicated in Fig. 9b, c, respectively), showing greater variations in ΔT with the panel placement. The stability of the water column was further examined by the gradient Richardson number to take shear stress into account. The increase in the Richardson number (Fig. 8c, d) indicates an increased stability under the panel. The increased thermal stability is compounded by the reduction of wind stress on the water surface, which has the effect of reducing mixing energy. The overall impact of surficial heating and removal of wind stress caused by the placement of the panels results in an increase of the Richardson number from 2.3 to 3.3 and decrease in mixing energy by 2×10^{-7} from 9×10^{-7} to 7×10^{-7} W/kg averaged over the length of the longitudinal transect (Fig. 2b), respectively.

Further water quality parameters were averaged along the main axis of Tengeh and Poyan Reservoirs for the full year of 2016 in order to provide an estimate of the overall impacts on water quality. The model results for changes (difference in results with and without floating PV system) to TChla, DO, TN TP and TOC are shown in Fig. 10a–e. The differences are normalized by the average values without the PV system. In general, there is a net increase in TN and TP concentrations and reduction in TChla, DO and TOC values where the PV system is located, and virtually

unchanged elsewhere. The lower DO concentration under the solar panel, as predicted by the model, is consistent with YSI datasonde measurements (Fig. 5). The water surface beneath the panels is subject to light limiting conditions, inhibiting photosynthesis. This leads to a decrease in TChla concentration by about 20% at the surface and 30% near the bottom. Respiration and a less well-mixed water column, on the other hand, result in a reduction of DO throughout the water column; DO at the surface decreases by about 30% and by about 50% at the bottom. Due to increased stability conditions, the mixing of DO from the surface waters to the bottom layers is dampened, resulting in decreased DO concentrations at greater depths. DO concentrations directly underneath the panels are noticed to drop to about 2 mg/L. In addition, TOC concentrations decrease by about 15% under the panels. The increase in TN and TP concentrations (Fig. 10c, d) and accompanying reduction in TChla and DO also are attributed to decreased metabolism and nutrient uptake by algae, caused by decreased light penetration as a result of shielding. TP and TN increase by 30% and 10%, respectively, averaged over the water column under PV panels. In the vicinity of PV panels (in the area from L2 to L1), TP increases by 20% and TN increases by roughly 5% over the water column.

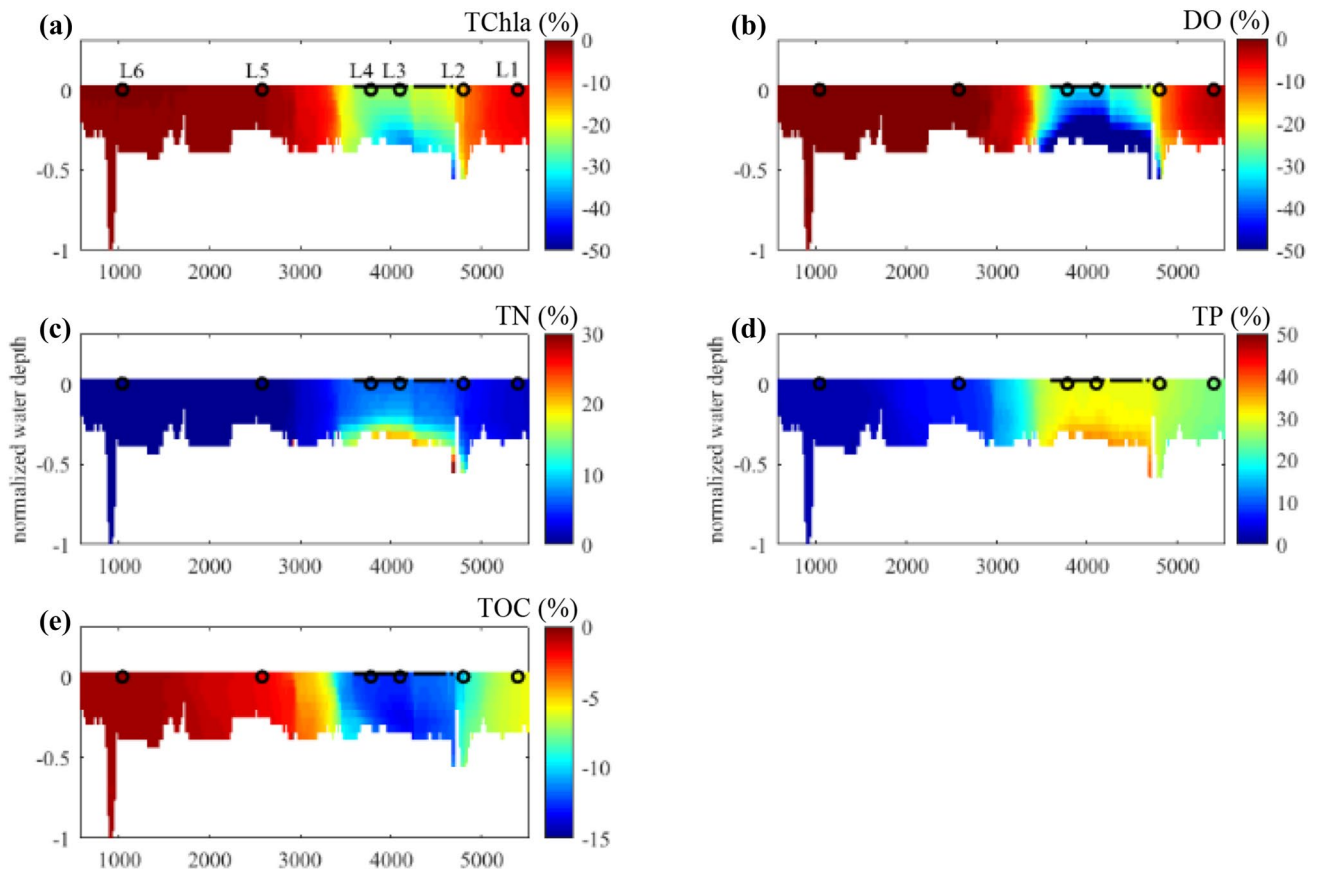


Fig. 10 Percentage change in selected water quality parameters averaged for 2016, normalized by average concentrations for (a) TChla, (b) DO, (c) TN, (d) TP and (e) TOC along the longitudinal transect

(Fig. 1b). The solid black lines on the water surface adjoining L2 to L4 represent approximate location of the floating PV panels.

Conclusions and recommendations

We investigated the influence of a floating PV system on water quality at the Tengeh and Poyan Reservoirs, Singapore, through a combination of opportunistic and continuous field sampling and numerical modelling. Additional radiometer measurements were made under the solar panels. The study is significant as it was the first such monitoring and modelling work of its kind. The following conclusions can be drawn from this study: (i) The field study shows the increase in surface water temperature by 0.5 °C on average, pH value increase by 0.5, DO reduction by about 2 mg/L under the 1 ha demonstration panels. Scale effects were observed, i.e. the changes are also supported by smaller panels (6 m² PV system) where the change was less than for a 1 ha demonstration floating PV system. (ii) The radiometer measurements indicate that net radiation decreased, of which the shortwave radiation was significantly reduced by the floating PV panels, but the net long-wave radiation increased due to re-radiation by the panels

placed above the water surface. The temperature of the air layer below the PV panels increased by about 4 °C on average in the daytime but reduced close to ambient conditions in the night. The warming of the air layer was driven by heating from the panels. (iii) There is overall good agreement between field and model results. Numerical modelling highlighted a significant decrease in chlorophyll *a* and in dissolved oxygen due to light limiting conditions and increased nutrient concentrations in the water column associated with an attendant decrease in chlorophyll *a* concentrations beneath the panels. An increase in water column stability associated with a shift in energy budget and reduced wind mixing further reducing dissolved oxygen concentrations, enhancing nutrient accumulation near the reservoir bottom, are noted as key consequences to panel coverage of the reservoir surface. Distant from the PV panels, water temperature, stability and water quality remain unaffected in Poyan Reservoir. (iv) Our study provides a high level of environmental assessment associated with floating PV systems, which has not previously been done and suggests a methodology for future investigations. To

our knowledge, this is the first modelling effort of its kind to explore the impact of floating PV systems. The field sampling is integral to providing verification to the model results and part of the model predictions. This is a preliminary study on the water quality in a freshwater body before the actual full-scale floating PV farm was installed. As a result of this study, measurements including surface–bottom water temperature difference and surface and bottom sampling for water quality at the panel location should be implemented. Further modelling needs to be carried out to investigate other panel configurations and coverage.

Supplementary Information The online version contains supplementary material available at <https://doi.org/10.1007/s10201-022-00698-y>.

Acknowledgements Funding received from PUB, Singapore’s National Water Agency for the Project Study of the Environmental Effects of Floating Solar Panels in Tengah Reservoir—Water Quality Impacts, is gratefully acknowledged. Mr Syed Alwi Bin Sheikh Bin Hussien Alkaff assisted with the field sampling work. Dr Le Song Ha and Dr Pennan Chinnasamy assisted with the initial catchment modelling work predicting catchment flows and loadings to be used as inputs to the ELCD model. This catchment model work was subsequently completed by Dr Josh Ho Huu Loc. Their contributions are gratefully acknowledged. Kim Irvine was on a Bualuang ASEAN Fellowship, while this manuscript was written. To the best of our knowledge, this study was conducted in compliance with applicable ethical standards and laws.

Funding Open Access funding enabled and organized by CAUL and its Member Institutions.

Open Access This article is licensed under a Creative Commons Attribution 4.0 International License, which permits use, sharing, adaptation, distribution and reproduction in any medium or format, as long as you give appropriate credit to the original author(s) and the source, provide a link to the Creative Commons licence, and indicate if changes were made. The images or other third party material in this article are included in the article’s Creative Commons licence, unless indicated otherwise in a credit line to the material. If material is not included in the article’s Creative Commons licence and your intended use is not permitted by statutory regulation or exceeds the permitted use, you will need to obtain permission directly from the copyright holder. To view a copy of this licence, visit <http://creativecommons.org/licenses/by/4.0/>.

References

- Akaike H (1969) Fitting autoregressive models for prediction. *Ann Inst Stat Math* 21:243–247. <https://doi.org/10.1007/BF02532251> [APHA] American Public Health Association (2005) Standard methods for the examination of water and wastewater. Washington (DC).
- Armstrong S, Hurley WG (2010) A thermal model for photovoltaic panels under varying atmospheric conditions. *Appl Therm Eng* 30(11):1488–1495. <https://doi.org/10.1016/j.applthermaleng.2010.03.012>
- Boh S (2016) World’s largest floating solar photovoltaic cell test-bed launched in Singapore. <https://www.straitstimes.com/singapore/worlds-largest-floating-solar-photovoltaic-cell-test-bed-launched-in-singapore>
- Boothroyd IKG, Quinn JM, Langer ER, Costley KJ, Steward G (2004) Riparian buffers mitigate effects of pine plantation logging on New Zealand streams: 1. Riparian vegetation structure, stream geomorphology and periphyton. *Forest Ecol Manag* 194(1–3):199–213. <https://doi.org/10.1016/j.foreco.2004.02.018>
- Boyd J (2016) Japan Building World’s Largest Floating Solar Power Plant, *IEEE Spectrum*. <https://spectrum.ieee.org/energywise/energy/renewables/japan-building-worlds-largest-floating-solar-power-plant>.
- Chen X, He S, Huang Y, Kong H, Lin Y, Li C, Zeng G (2009a) Laboratory investigation of reducing two algae from eutrophic water treated with light-shading plus aeration. *Chemosphere* 76(9):1303–1307. <https://doi.org/10.1016/j.chemosphere.2009.05.027>
- Chen X, Kong H, He S, Wu D, Li C, Huang X (2009b) Reducing harmful algae in raw water by light-shading. *Process Biochem* 44(3):357–360. <https://doi.org/10.1016/j.procbio.2008.11.002>
- Davies-Colley RJ, Quinn JM (1998) Stream lighting in five regions of North Island, New Zealand: control by channel size and riparian vegetation. *New Zeal J Mar Fresh* 32(4):591–605. <https://doi.org/10.1080/00288330.1998.9516847>
- Ellabban O, Abu-Rub H, Blaabjerg F (2014) Renewable energy resources: current status, future prospects and their enabling technology. *Renew Sust Energ Rev* 39:748–764. <https://doi.org/10.1016/j.rser.2014.07.113>
- Fischer HB (1979) *Mixing in inland and coastal waters*. Academic Press, New York
- Ghermandi A, Vandenberghe V, Benedetti L, Bauwens W, Vanrolleghem PA (2009) Model-based assessment of shading effect by riparian vegetation on river water quality. *Ecol Eng* 35(1):92–104. <https://doi.org/10.1016/j.ecoleng.2008.09.014>
- Haas J, Khalighi J, de la Fuente A, Gerbersdorf SU, Nowak W, Chen PJ (2020) Floating photovoltaic plants: ecological impacts versus hydropower operation flexibility. *Energy Convers Manage* 206:112414. <https://doi.org/10.1016/j.enconman.2019.112414>
- Hanwha (2017) Hanwha to Build World’s Largest Floating Solar Farm, https://www.hanwha.com/en/news_and_media/press_release/hanwha-to-build-worlds-largest-floating-solar-farm.html
- Harvey F (2016) World’s biggest floating solar farm powers up outside London, *The Guardian*, <https://www.theguardian.com/environment/2016/feb/29/worlds-biggest-floating-solar-farm-power-up-outside-london>
- Hipsey MR, Sivapalan M, Clement TP (2004) A numerical and field investigation of surface heat fluxes from small wind-sheltered waterbodies in semi-arid Western Australia. *Environ Fluid Mech* 4(1):79–106. <https://doi.org/10.1023/a:1025547707198>
- Huisman J, Sharples J, Stroom JM, Visser PM, Kardinaal WEA, Verspagen JMH, Sommeijer B (2004) Changes in turbulent mixing shift competition for light between phytoplankton species. *Ecology* 85(11):2960–2970. <https://doi.org/10.1890/03-0763>
- International Energy Agency (2017) <https://www.iea.org/publications/renewables2017/#section-1>.
- Irvine KN, McCorkhill G, Caruso J (2005) Continuous monitoring of conventional parameters to assess receiving water quality in support of combined sewer overflow abatement plans. *Water Environ Res* 77(5):543–552
- Irvine KN, Sovann C, Suthipong S, Kok S, Chea E (2015) Application of PCSWMM to assess wastewater treatment and urban flooding scenarios in Phnom Penh, Cambodia: a tool to support eco-city planning. *J Water Manag Model*. 2:2. <https://doi.org/10.14796/JWMM.C389>
- Jayasooriya VM, Ng AWM (2014) Tools for modeling of stormwater management and economics of green infrastructure practices: a review. *Water Air Soil Poll* 225(8):2055. <https://doi.org/10.1007/s11270-014-2055-1>

- Laval B, Imberger J, Hodges BR, Stocker R (2003) Modeling circulation in lakes: spatial and temporal variations. *Limnol Oceanogr* 48(3):983–994. <https://doi.org/10.4319/lo.2003.48.3.0983>
- Leon LF, Smith REH, Hipsey MR, Bocaniov SA, Higgins SN, Hecky RE, Antenucci JP, Imberger JA, Guildford SJ (2011) Application of a 3D hydrodynamic–biological model for seasonal and spatial dynamics of water quality and phytoplankton in Lake Erie. *J Great Lakes Res* 37(1):41–53. <https://doi.org/10.1016/j.jglr.2010.12.007>
- [NEA] National Environment Agency, Singapore (2016) <https://www.nea.gov.sg/media/advisories/advisories/warmer-and-drier-conditions-with-the-onset-of-southwest-monsoon>
- Niazi M, Nietch C, Maghrebi M, Jackson N, Bennett BR, Tryby M, Massoudieh A (2017) Storm water management model: performance review and gap analysis. *J Sust Water Built Environ* 3(2):04017002
- Oswald CJ, Rouse WR (2004) Thermal characteristics and energy balance of various-size canadian shield lakes in the mackenzie river Basin. *J Hydrometeorol* 5(1):129–144
- [PUB] PUB, Singapore's National Water Agency (2017) PUB studying clean energy solutions for blue spaces. <https://www.pub.gov.sg/news/pressreleases/pubstudyingcleanenergysolutionsfrombluespaces>
- [PUB] PUB, Singapore's National Water Agency (2018) PUB looks to Bedok and Lower Seletar Reservoirs for more solar power, Singapore. <https://www.pub.gov.sg/news/pressreleases/publookstobedokandlowerseletarreservoirsformoresolarpower>
- Ren R (2016) Global status report. Renewable energy policy network for the 21st century. https://www.ren21.net/wp-content/uploads/2019/05/REN21_GSR2016_FullReport_en_11.pdf, accessed 23 Dec 2019.
- Rueda F, Schladow SG, Monismith S, Stacey M (2005) On the effects of topography on wind and the generation of currents in a large multi-basin lake. *Hydrobiologia* 532(1–3):139–151
- Sahu A, Yadav N, Sudhakar K (2016) Floating photovoltaic power plant: a review. *Renew Sust Energ Rev* 66:815–824. <https://doi.org/10.1016/j.rser.2016.08.051>
- Soh A (2017) Singapore scales up floating solar PV ambitions, The Business Times, <https://www.businesstimes.com.sg/energy-commodities/singapore-scales-up-floating-solar-pv-ambitions>
- Song JY, Chung ES (2017) A multi-criteria decision analysis system for prioritizing sites and types of low impact development practices: case of Korea. *Water* 9(4):291. <https://doi.org/10.3390/w9040291>
- Trapani K, Redón Santafé M (2015) A review of floating photovoltaic installations: 2007–2013. *Prog Photovolt* 23(4):524–532. <https://doi.org/10.1002/pip.2466>
- Xing Z, Chua LHC, Miao H, Imberger J, Yang P (2018) Wind shielding impacts on water quality in an urban reservoir. *Water Resour Manag* 32:3549–3561. <https://doi.org/10.1007/s11269-018-1980-y>
- Yang P, Fong DA, Lo EYM, Monismith SG (2019a) Circulation patterns in a shallow tropical reservoir: Observations and modeling. *J Hydro-Environ Res* 27:75–86. <https://doi.org/10.1016/j.jher.2019.09.002>
- Yang P, Fong DA, Lo EYM, Monismith SG (2019b) Vertical mixing in a shallow tropical reservoir. *Limnology* 20:279–296. <https://doi.org/10.1007/s10201-019-00577-z>
- Yang P, Chua LHC, Irvine KN, Imberger J (2021) Radiation and energy budget dynamics associated with a floating photovoltaic system. *Water Res*. <https://doi.org/10.1016/j.watres.2021.117745>
- Yin K, Lin Z, Ke Z (2004) Temporal and spatial distribution of dissolved oxygen in the Pearl River Estuary and adjacent coastal waters. *Cont Shelf Res* 24(16):1935–1948. <https://doi.org/10.1016/j.csr.2004.06.017>
- Zsiborács H, Pályi B, Pintér G, Popp J, Balogh P, Gabnai B (2016) Technical-economic study of cooled crystalline solar modules. *Sol Energy* 140:227–235. <https://doi.org/10.1016/j.solener.2016.11.009>

Publisher's Note Springer Nature remains neutral with regard to jurisdictional claims in published maps and institutional affiliations.